

METHOD TO IDENTIFY IF TORSIONAL MODE OF A BUILDING IS ITS FIRST MODE

G. Tamizharasi¹ and C.V.R. Murty²

(Submitted April 2023; Reviewed May 2023; Accepted January 2024)

ABSTRACT

Torsionally flexible buildings (that have *torsional mode* as fundamental mode) twist during earthquake shaking, and may *collapse partially* or *completely* depending upon the direction and level of shaking. The problem is aggravated when the building is *torsionally unsymmetrical*. Some design codes (like *Eurocode*, *Indian Code*) explicitly prohibit the design of such buildings. This paper presents a simple approximate method to identify torsionally flexible *RC Moment Frame* and *RC Structural Wall* buildings at the *initial proportioning* stage itself without carrying out a detailed structural analysis. It is possible to identify whether or not the first mode is torsional mode of a building (*i.e.*, torsionally flexible building) if *Natural Period Ratio* $\tau > 1$ by modelling the building with rigid diaphragm and distribution of mass & stiffness along the height of building, and estimating: (1) radius of gyration of rotational mass r_m of each floor plan geometry by lumping the masses of slabs, beams and all vertical elements at each nodes, (2) radius of gyration of twisting stiffness $r_{K\theta}$ of all vertical elements using their translational and torsional stiffnesses (considering flexibility of adjoining beams and vertical elements accounting for both flexural and shear deformations), and (iv) τ ($=r_m/r_{K\theta}$). The method is validated with *3D Modal Analysis* (using $\tau = T_\theta/T$, where T_θ is *Uncoupled Torsional Natural Period* and T *Uncoupled Translational Natural Period*) of hypothetical buildings using a commercial structural analysis software. Also, parameters are identified that lead to $\tau > 1$, and solutions suggested to avoid torsional flexibility in buildings. Further, the method helps identify *vertical stiffness irregularity* in buildings. Draft provisions are suggested for inclusion in seismic codes. Also, poor performance of multi-storey building (with $\tau > 1$) is demonstrated using nonlinear static and nonlinear time history analyses.

<https://doi.org/10.5459/bnzsee.1645>

INTRODUCTION

Usually, poor performance of buildings under earthquake shaking arises from their poor configuration in plan and elevation. The negative effects induced in buildings due to poor plan configurations are predominantly due to *torsional effects*, *re-entrant corners*, and *flexible floor diaphragms*. Torsional effects in buildings cause lateral-torsional response in buildings under earthquake shaking; normalised displacement response amplification depends on structural parameters like normalised torsional eccentricity e_k/B , natural period ratio τ , normalised radius of gyration of rotational mass r_m/B [1]. Most building code provisions seek design for torsional eccentricity and define torsionally regular buildings using relative edge displacements. e_k/B accounts for the asymmetry that arise in buildings due to location of *Center of Mass CM* and *Center of Resistance CR*, τ accounts for the overall distribution of mass and stiffness in plan (and helps in the identification of torsionally flexible buildings), and r_m/B accounts for mass distribution in plan of various plan geometries (like L, T, V, Y and H; which is usually expressed in terms of plan aspect ratio for rectangular buildings).

In addition, buildings with poor plan geometry induce lateral-torsional response and cause significant stress concentration near re-entrant corners [2,3]. Therefore, building code provisions place limits on re-entrant corners using: (a) normalised projection dimension with overall plan dimension in considered direction (*e.g.*, ASCE 7-16, India, Mexico, Iran, and Peru), or (b) normalised area of projection with gross area of building plan (*e.g.*, Eurocode 8). This effect can be reduced by providing uniform distribution of mass and stiffness per unit area. The provisions given for torsion in building code

provisions are applicable to buildings with rigid floor diaphragms. The criteria for rigid floor diaphragms are expressed usually in terms of plan aspect ratio, percentage of openings and relative edge displacements. But, the effect due to floor flexibility is prominent in buildings with poor plan geometry, which induces oscillation of individual wings; sometimes, it may cause serious effects of pounding damages in buildings [4]. In all, the negative effects on buildings due to poor plan configuration should be avoided at the preliminary design stage itself. This study focuses on only containing torsional effects in buildings.

Mostly, poor performances of many buildings in past earthquakes due to torsion have been attributed to two causes, namely: (a) *torsionally unsymmetrical buildings* (having large torsional eccentricity), and (b) *torsionally flexible buildings* (having torsional mode as their fundamental mode with large mass participation (say 70% or more) in rotation). Failure of such buildings is brittle without much warning. When such buildings twist, they impose increased lateral displacement demand on the perimeter columns. If these columns do not have sufficient translational displacement ductility, they fail, thereby causing *partial* or *complete* collapse. For example, buildings with stiff core at center and irregular plan geometry can undergo *partial collapse* owing to perimeter columns not being ductile, while it can undergo complete collapse (with structural wall core standing without any damage) owing to large plan aspect ratio (Figure 1) [5-8]. Most studies conducted so far addressed behaviour of *torsionally unsymmetrical buildings*; only a few of them studied behaviour of *torsionally flexible buildings*. Hence, the present study examines *torsionally flexible buildings*. Usually, poor performances of these buildings originate from poor structural configuration in plan, *e.g.*, those

¹ Corresponding Author, Assistant Professor, Sardar Vallabhbhai National Institute of Technology, India, gtamizh@amd.svnit.ac.in

² P. S. Rao Institute Chair Professor, Indian Institute of Technology Madras, India, cvr@iitm.ac.in

with structural wall core at center, large plan aspect ratio, and/or poor plan geometry. The effects are worsened if the building is torsionally unsymmetrical [3, 9-10]. Therefore, it is important to identify *torsionally flexible buildings* at the preliminary design stage itself, and avoid them.

The Natural Period Ratio τ is used to define *torsionally flexible buildings* and given by:

$$\tau = \frac{T_\theta}{T} = \frac{r_m}{r_{K\theta}} \quad (1)$$

where T_θ is the uncoupled torsional natural period, T the uncoupled translational natural period, r_m the radius of gyration of rotational mass and $r_{K\theta}$ the radius of gyration of twisting stiffness. τ reflects the mass and stiffness distribution in plan. A building is *torsionally flexible* when $\tau > 1$, and *torsionally stiff* when $\tau < 1$. Torsionally stiff buildings have translational mode as their fundamental mode and with large mass participation (say 70% or more) in translation. τ can be estimated using either T_θ and T (requiring structural analysis of the building by 3D Modal Analysis (3D MA) using commercial software, say SAP2000 or ETABS), or r_m and $r_{K\theta}$ (without requiring structural analysis by any 3D MA, but by using simple analytical methods). To estimate r_m and $r_{K\theta}$, an estimate of seismic mass m and seismic mass moment of inertia I^M (of building plan and lateral structural elements), translational stiffness K and torsional stiffness K_θ (of lateral structural elements at each storey) is required. Estimating m and I^M is straight forward by lumping masses at each node but estimating K and K_θ is not. Analytical methods have been proposed in literature to estimate K and K_θ [11, 12], requiring simple hand calculations or complete 3D modelling of buildings using softwares. Not all these methods account for variation of stiffness along the height of buildings; one method is available to identify torsional flexibility [13].

The main intent of this paper is to estimate τ ($=T_\theta/T_x$). Thus, efforts are made to see if simple methods can identify torsionally flexible buildings (with $\tau > 1$) at the pre-design stage before performing structural analysis on standard software. The importance of the efficacy of the simple models suggested in this paper is that they can be used in the pre-design stage by architects to finalise the structural system and in initial proportioning of buildings without doing any computer modelling of the structures. The use of these simple methods permits more iterations when choosing structural systems, and hence saves a lot of time of the architects and designers.

This paper presents a method (with *Step-By-Step Procedure*) to identify two effects in buildings, namely: (a) torsionally flexibility, and (b) vertically irregularity. It is validated through analytical study conducted on a spectrum of building configurations using elastic 3D MA. Critical parameters are identified, which affect both *torsional flexibility* and *vertical*

irregularity, and possible solutions recommended for overcoming the same.

PROPOSED METHOD

Usually, methods using single-storey buildings seldom predict the variation of stiffness distribution along the height of buildings. Therefore, in present study, modification factors are proposed to account for the same. The proposed method is applicable directly to *multi-storey* buildings but with modification factors applied to *single-storey* buildings. Analytical methods (of single-storey or multi-storey) are explained in detail considering a typical storey i of the building. Floor diaphragm is assumed to be rigid with uniform mass distribution. The effect of non-uniform distribution of mass or varying plan geometry is considered by lumping masses at required nodal locations. Also, dimensions of vertical structural elements are considered uniform along the height of the building. CM is taken as the reference in the estimation of storey mass moment of inertia, storey stiffness and storey torsional stiffness, as its location does not vary under both elastic and inelastic actions.

A few code provisions (like Eurocode 8) define translational and torsional stiffnesses with respect to *Center of Stiffness CS* or *Center of Resistance CR*. But, CM is considered in present study as the mathematical representations do not change the system characteristics. The following is the *step-by-step procedure* employed to identify torsional flexibility of buildings:

Step 1: Estimate seismic mass m_i lumped at CM at storey i and seismic mass moment of inertia I_i^M of storey i about the CM

Consider an analytical model of a building with general plan geometry (Figure 2). The masses of slabs and beams are lumped in plan at the nodes at each floor, and of vertical structural elements are lumped along the elevation, one half to the node above and below that storey. The locations of nodes are defined with respect to the Center of Mass CM of that floor. The building is idealised along its height to have *two translational degrees of freedom along X- and Y- directions, and a torsional degree of freedom* at each floor. To estimate the mass moment of inertia, the *rotational characteristics* of the building are considered. Thus, m_i and I_i^M are given by:

$$m_i = \sum_{j=1}^{n_{LM,i}} m_{i,j}, \text{ and} \quad (2)$$

$$I_i^M = \sum_{j=1}^{n_{VE,i}} I_{VEi,j}^M + \sum_{j=1}^{n_{LM,i}} m_{i,j} r_{i,j}^2. \quad (3)$$



Figure 1: Damage to torsionally flexible buildings owing to: (a) stiff core at center and irregular plan during 2001 Bhuj Earthquake, (b) brittle failure of perimeter columns of upper storeys during 1985 Mexico City Earthquake, and (c) large plan aspect ratio during 1985 Mexico City Earthquake [5-7].

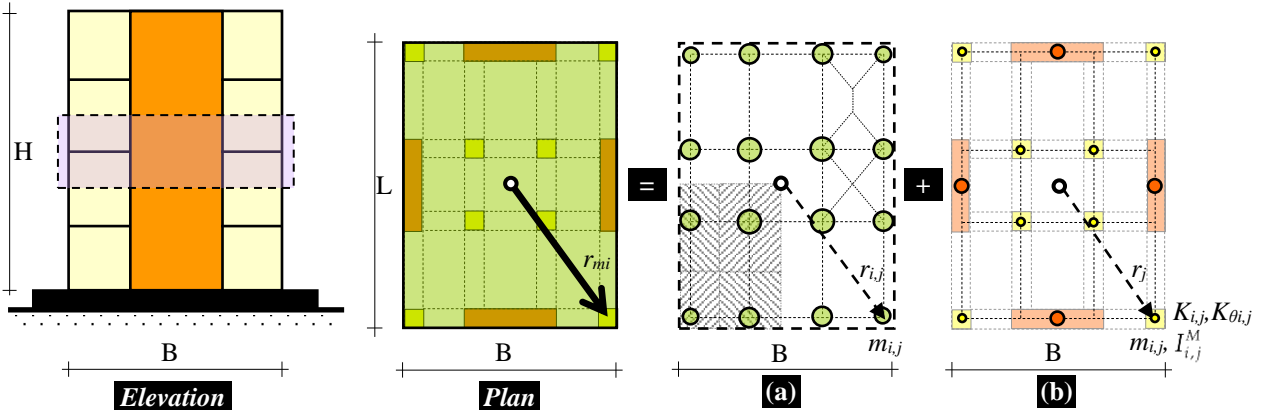


Figure 2: Typical floor plan of the analytical model of a building [13].

where $m_{i,j}$ is the seismic mass lumped at node j of the storey i , $I_{VEi,j}^M$ the seismic mass moment of inertia of vertical element at node j at i^{th} storey about its CG, $n_{LM,i}$ the number of lumped masses at node j of storey i , $n_{VE,i}$ the number of vertical element at node j of the storey i , and $r_{i,j}$ the distance from CM of the seismic mass lumped at node j of the storey i .

Step 2: Estimate storey translational stiffness K_{X_i} & K_{Y_i} along X - & Y - directions, and torsional stiffness K_{θ_i} about the CM at storey i

Five analytical methods (AMs) are used to estimate translational & torsional stiffnesses of lateral load resisting elements of multi-storey buildings, namely [13]:

1. AM1: Single isolated column of storey i :
 - (a) to estimate *in-plane translational* stiffness – fully restrained against *in-plane rotations* at the ends, and free to *translate in-plane* at the top (Figure 3(1)), and
 - (b) to estimate *torsional* stiffness – fully restrained against *in-plane rotation* and *in-plane translation* at the ends, and free to *twist* about the vertical axis but restrained against *in-plane rotation* and *in-plane translation* at the top, (Figure 4(1));
2. AM2: Storey sub-assembly of typical storey i of interior frame:
 - (a) to estimate *in-plane translational* stiffness – far ends of connecting beams & columns fully restrained against *in-plane rotation*, and free to *translate in-plane* at the top (Figure 3(2)), and
 - (b) to estimate *torsional* stiffness – far ends of connecting beams & columns fully restrained against *in-plane rotation* and *in-plane translation*, and free to *twist* about the vertical axis but restrained against *in-plane rotation* and *in-plane translation* at the top (Figure 4(2));
3. AM3: Storey sub-assembly of storey i of interior frame:
 - (a) to estimate *in-plane translational* stiffness – far ends of connecting beams & columns truncated at points of zero *in-plane* bending moment (mid-spans and mid-heights), and free to *translate in-plane* at the top (Figure 3(3)), and
 - (b) to estimate *torsional* stiffness – far ends of connecting beams & columns truncated at points of zero *in-plane* bending moment (mid-spans and mid-heights) and restrained against *in-plane translation*, model free to

twist about vertical axis, and model restrained against *in-plane translation* at the top (Figure 4(3)); and

4. AM4 and AM5: Stick model with mass lumped at each storey:
 - (a) to estimate *in-plane translational* stiffness – each floor node can *translate in-plane* but *cannot twist* about the vertical axis (Figure 3(4)), and
 - (b) to estimate *torsional* stiffness – each floor node *cannot translate in-plane* but can *twist* about the vertical axis (Figure 4(4)).

All these models are *unrestrained* at top against *in-plane* translation when estimating *translational stiffness* (Figure 3) and *fully restrained* at top against *in-plane* translation when estimating *torsional stiffness* (Figure 4). Methods AM1 to AM3 use expressions of K_{X_i} , K_{Y_i} and K_{θ_i} considering one storey at a time, without using software (named as *Set S*) given in literature [13]. AM1 ignores contribution of beam *in-plane* rotational flexibility by assuming zero joint rotation, *i.e.*, stiff joints. But, AM2 and AM3 consider *in-plane* rotational flexibility of adjoining beams; assumptions made are: (a) beams and columns undergo same *in-plane* rotation at each storey, (b) points of zero moments are at mid span/height, (c) beams are of same size in adjoining storeys above and below the storey considered, and (d) columns are of same size along the height of the building. Additionally, *in-plane* rotational degree of freedom is eliminated using static condensation in the estimation of translational stiffness.

In AM4, an idealised stick model is used with: (a) masses of each storey lumped at CM as equivalent mass and mass moment of inertia, and (b) stiffness of each storey lumped at CM as equivalent translational and torsional stiffnesses. Natural frequencies and mode shape vectors are used (of fundamental translational and torsional modes obtained from 3D MA of multi-storey buildings on software, named as *Set M*). All models consider *flexure and shear deformations* of structural elements, but ignore *axial deformations* [13].

In AM5 also, multi-storey buildings are idealised with idealised stick models. But, response quantities (like normalised storey forces, normalised storey torsional moments, normalised translational and rotational displacements about the CM) are used, which correspond to normalised *predominant translational and torsional modes of vibrations*. Then, *static equilibrium of storey forces & torsional moments* is employed corresponding to *in-plane translational & torsional displacements* about CM. This method resembles *Equivalent Static Approach (ESA) conducted on buildings* (e.g., [11]) for specific demand. AM5 does not require conducting separate ESA for *translational and torsional loads*, but requires estimates of response quantities using normalised predominant

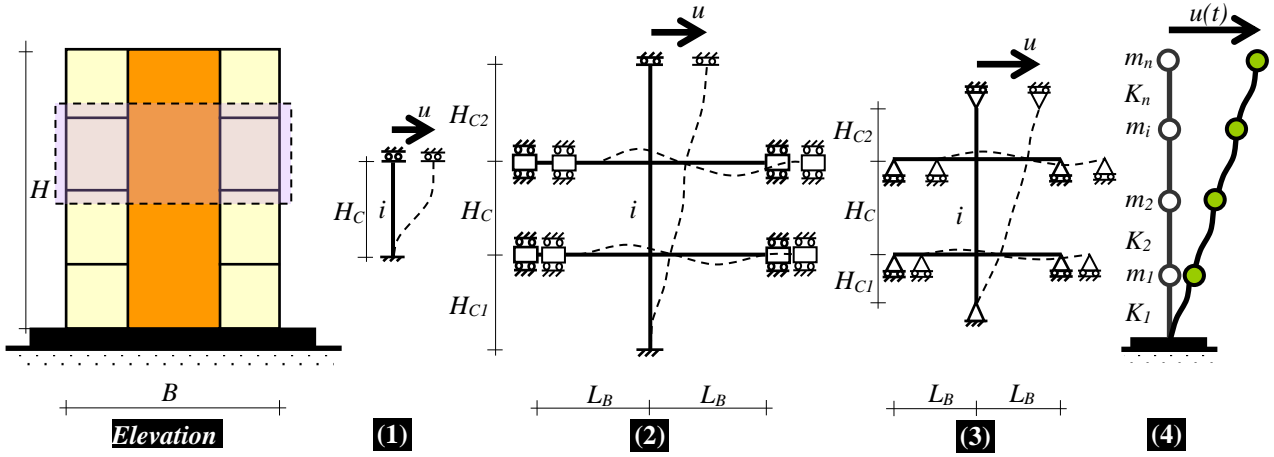


Figure 3: Idealisation of building employed in Analytical Methods to estimate in-plane translational storey stiffness: (1) AM1, (2) AM2, (3) AM3, (4) AM4 and AM5 [13].

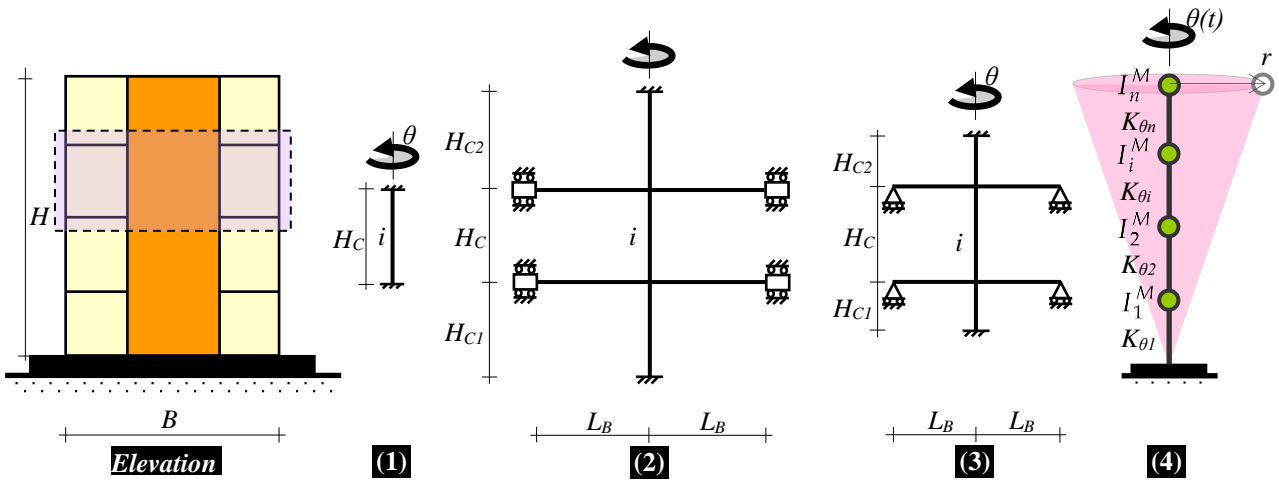


Figure 4: Idealisation of building employed in Analytical Methods to estimate torsional storey stiffness about the vertical axis: (1) AM1, (2) AM2, (3) AM3, (4) AM4 and AM5 [13].

independent translational and torsional modes of vibration. AM5 is used to validate τ_i at storey i estimated by AM4. Normalised storey forces F_i and normalised storey torsional moments $T_{\theta i}$ about CM are estimated corresponding to normalised storey translational Δ_i and normalised storey rotational θ_i modal displacements. Expressions for K_{X_i} , K_{Y_i} and $K_{\theta i}$ (Equations (4)-(6)) at storey i by different AMs are given in Table 1.

In AM4 and AM5, the 3D models of the buildings are considered. Hence, the actual condition will be captured – the building has *two-way moment frames* (normally used in concrete buildings) or *one-way moment frames* (becoming increasingly common in steel buildings). The suggested method is general enough to capture both cases.

Step 3: Estimate modified translational stiffness K_{MX_i} & K_{MY_i} along X & Y-directions, and modified torsional stiffness $K_{M\theta i}$

m_i and I_i^M estimated at each storey are same from AM1 to AM4. Hence, mass distribution remains same for Set S and Set M. But, AM1 to AM3 do not reflect the variation of lateral storey stiffness along the height of buildings, even after considering the varying boundary conditions at base and top stories, unlike in AM4. Therefore, modification factors are suggested to use estimates of translational and torsional stiffnesses from AM1 to AM3 to match the results of AM4 (i.e., Set S with Set M), to incorporate the effect of stiffness

distribution along the height of the buildings. These modification factors for translational stiffnesses M_{FX_i} & M_{FY_i} and for torsional stiffness $M_{F\theta i}$ at storey i are:

$$M_{FX_i} = \frac{K_{X1}}{K_{X_i}}, \quad (7)$$

$$M_{FY_i} = \frac{K_{Y1}}{K_{Y_i}}, \text{ and} \quad (8)$$

$$M_{F\theta i} = \frac{K_{\theta 1}}{K_{\theta i}}. \quad (9)$$

Using Equations (7) to (9), the modification factors are obtained as the ratio of lateral (*translational or torsional*) stiffness of each storey (estimated independently considering one storey at a time) using AM1 to AM3 and lateral (*translational or torsional*) stiffness at each storey i estimated using AM4. Modification factor thus obtained, accounts for the variation of lateral (*translational or torsional*) stiffness variation along the height of building. This factor is used to normalise the estimated lateral (*translational or torsional*) stiffness considering one storey at a time using AM1 to AM3. Thus, modified lateral translational stiffnesses K_{MX_i} & K_{MY_i} and torsional stiffness $K_{M\theta i}$ at storey i are:

$$K_{MX_i} = \frac{K_{X1}}{M_{FX_i}}, \quad (10)$$

Table 1: Expressions of K_{Xi} , K_{Yi} and $K_{\theta i}$ at storey i by five analytical methods.

S.No.	Quantity	Set S		Set M		Eq.
		AM1 to AM3		AM4	AM5	
1	K_{Xi}	$\sum_{j=1}^{n_{VEX,i}} K_{Xi,j}$, $i=1$		$\left[\frac{\omega_{Xn}^2 \sum_{i=1}^N m_i \phi_{X,i}}{(\phi_{X,i} - \phi_{X,i-1})} \right]$	$\left[\frac{F_{Yi}}{(\Delta_{Yi} - \Delta_{Y(i-1)})} \right]$	(4)
2	K_{Yi}	$\sum_{j=1}^{n_{VEY,i}} K_{Yi,j}$, $i=1$		$\left[\frac{\omega_{Yn}^2 \sum_{i=1}^N m_i \phi_{Y,i}}{(\phi_{Y,i} - \phi_{Y,i-1})} \right]$	$\left[\frac{F_{Yi}}{(\Delta_{Yi} - \Delta_{Y(i-1)})} \right]$	(5)
3	$K_{\theta i}$	$\sum_{j=1}^{n_{VE,i}} K_{\theta,j} + \sum_{j=1}^{n_{VEX,i}} K_{Xi,j} y_{i,j}^2 + \sum_{j=1}^{n_{VEY,i}} K_{Yi,j} x_{i,j}^2$, $i=1$		$\left[\frac{\omega_{\theta n}^2 \sum_{i=1}^N I_i^M \phi_{\theta}}{(\phi_{\theta} - \phi_{\theta(i-1)})} \right]$	$K_{\theta} = \left[\frac{T_{\theta}}{(\theta_i - \theta_{i-1})} \right]$	(6)

Note:

$$F_{Xi} = \sum_{j=1}^{n_{VEX,i}} F_{Xi,j}, \quad F_{Yi} = \sum_{j=1}^{n_{VEY,i}} F_{Yi,j} \quad \text{and} \quad T_i = \sum_{j=1}^{n_{VE,i}} T_{\theta,j} + \sum_{j=1}^{n_{VEX,i}} F_{Xi,j} y_{i,j} + \sum_{j=1}^{n_{VEY,i}} F_{Yi,j} x_{i,j},$$

where

- F_{Xi} = Storey shear about the CM of the storey i for loading along X-direction;
 F_{Yi} = Storey shear about the CM of the storey i for loading along Y-direction;
 $T_{\theta i}$ = Torsional moment about the CM of the storey i ;
 $F_{Xi,j}$ = Lateral force of vertical element at node j of the storey i along X-direction;
 $F_{Yi,j}$ = Lateral force of vertical element at node j of the storey i along Y-direction; and
 $T_{\theta,j}$ = Torsional moment of vertical element at node j of the storey i about its CG.
 K_{X1} = Storey translational stiffness of considered single-storey of the building along X-direction;
 K_{Y1} = Storey translational stiffness of considered single-storey of the building along Y-direction;
 $K_{\theta 1}$ = Storey torsional stiffness about the CM of considered single-storey of the building;
 $K_{Xi,j}$ = Lateral translational stiffness of vertical element at node j of storey i along X-direction;
 $K_{Yi,j}$ = Lateral translational stiffness of vertical element at node j of storey i along Y-direction;
 $K_{\theta,j}$ = Torsional stiffness of vertical element j at i^{th} storey about its CG;
 N = Total number of storeys;
 $n_{VEX,i}$ = Number of vertical element at node j of the storey i along X-direction;
 $n_{VEY,i}$ = Number of vertical element at node j of the storey i along Y-direction;
 $x_{i,j}$ = Distance from CM of the vertical element at node j of storey i along X-direction;
 $y_{i,j}$ = Distance from CM of the vertical element at node j of storey i along Y-direction;
 Δ_{Xi} = Lateral translational displacement about the CM of the storey i for shaking along X-direction;
 Δ_{Yi} = Lateral translational displacement about the CM of the storey i for shaking along Y-direction;
 ω_{Xn} = Translational natural frequency of n^{th} mode of vibration along X-direction;
 ω_{Yn} = Translational natural frequency of n^{th} mode of vibration along Y-direction;
 $\omega_{\theta n}$ = Torsional natural frequency of n^{th} mode of vibration along θ -direction;
 $\phi_{X,i}$ = Translational mode shape vector of n^{th} mode of vibration along X-direction;
 $\phi_{Y,i}$ = Translational mode shape vector of n^{th} mode of vibration along Y-direction;
 $\phi_{\theta,i}$ = Torsional mode shape vector of n^{th} mode of vibration along θ -direction; and
 θ_i = Rotation about the CM of the storey i .

$$K_{MYi} = \frac{K_{Y1}}{M_{FYi}}, \text{ and} \quad (11)$$

$$K_{M\theta i} = \frac{K_{\theta 1}}{M_{F\theta i}}. \quad (12)$$

Alternately, the modification factors shall be obtained by assuming a linear lateral translational and torsional mode shapes in the initial design stage and applied to single-storey models; but it requires a detailed study.

Step 4: Estimate radius of gyration of rotational mass r_{mi} and radius of gyration of twisting stiffness $r_{K\theta i}$ of storey i

The radius r_{mi} of gyration of rotational mass is estimated as:

$$r_{mi} = \sqrt{\frac{I_i^M}{m_i}}. \quad (13)$$

Radius of gyration of twisting stiffness is estimated using translational and torsional stiffnesses of vertical elements, which is contributed by beams, columns and structural walls. It represents the *geometric distribution* of lateral load resisting elements in plan (like distribution of mass) of these elements (Figure 2). Thus, the radii of gyration of twisting stiffnesses $r_{K\theta_{Xi}}$ and $r_{K\theta_{Yi}}$ of storey i along X- and Y-directions are estimated as:

$$r_{K\theta_{Xi}} = \sqrt{\frac{K_{\theta i}}{K_{Xi}}}, \text{ and} \quad (14)$$

$$r_{K\theta_{Yi}} = \sqrt{\frac{K_{\theta i}}{K_{Yi}}}. \quad (15)$$

Equations (14) and (15) are applicable for all analytical methods. When modification factors are used for *Set S*, then the estimation of radii of gyration of twisting stiffnesses, K_{Xi} , K_{Yi} and $K_{\theta i}$, shall be replaced by K_{MXi} , K_{MYi} and $K_{M\theta i}$ (*i.e.*, Equations (10)-(12)).

Step 5: Estimate natural period ratio τ of each storey

τ defines torsional flexibility of the building considering overall distribution of mass and stiffness along the height of building. It is obtained using results of 3D MA using T_{θ}/T , uncoupled torsional T_{θ} and uncoupled translational T natural periods. Estimating τ_i at each storey will help understanding the distribution of mass and stiffness at each storey (using $r_m/r_{K\theta}$). Alternately, it helps identifying the variation of mass and stiffness distribution along the height of building. AM4 and AM5 provide τ_i at each storey (*Set M*), while AM1 to AM3 estimates τ_i considering one storey at a time (*SET S*), and shall be modified with factors to account for stiffness variation (and becomes *Set M*). Finally, mean value of *Set M* shall be used to compare with results of 3D MA. Natural period ratios τ_{Xi} and τ_{Yi} of storey i along X- and Y-directions are given by:

$$\tau_{Xi} = \frac{T_{\theta}}{T_X} = \frac{r_{mi}}{r_{K\theta_{Xi}}}, \text{ and} \quad (16)$$

$$\tau_{Yi} = \frac{T_{\theta}}{T_Y} = \frac{r_{mi}}{r_{K\theta_{Yi}}}. \quad (17)$$

where T_X is the uncoupled translational natural period of the building along X-direction, T_Y the uncoupled translational natural period of the building along Y-direction, and T_{θ} the uncoupled torsional natural period. Finally, a building is identified to be *torsionally flexible* when $\tau > 1$, and *torsionally stiff* when $\tau < 1$.

NUMERICAL STUDY

Validation of Proposed Method Using Single and Multi-storey Buildings

It is known that buildings with irregular plan geometries (alphabet shaped buildings) have *large eccentricity* between center of mass and center of resistance. Also, it is known that they will twist even under unidirectional ground motion; the proximity of τ to 1.0 (or even exceedance of τ over 1.0) is expected in *all cases*. Here, this twist needs to be arrested with more serious actions are needed by the designer, in terms of consciously balancing the stiffness in plan according to the mass along each plan direction. But, the more challenging situation is to identify which buildings with regular overall plan geometries twist. Hence, this study devotes more attention to this aspect of regular buildings with simple plan geometries with uniform mass and stiffness distribution and rigid diaphragms; the proximity of τ to 1.0 is *not obvious* in many cases.

10-storey RC buildings (with fixed base) of different structural configurations in plan (Figure 5) are considered to estimate τ using all five AMs. These configurations include buildings with moment frames, with structural walls, and with frames and structural walls. The cases considered include: (i) size and shape of vertical elements, (ii) plan aspect ratio (L/B) of the building in the range 1 to 3, where L is the longitudinal plan dimension and B the lateral plan dimension, and (iii) structural walls along one, and along two principal plan directions. The effect of slenderness ratio (H/B), *i.e.*, height to lateral dimension ratio, is reported elsewhere [13]. These building configurations (*BCs*) have 4m bay length in each direction and 3m floor height. Column sizes are: (i) 500mm × 500mm and 300mm × 500mm in frame buildings, and (ii) 400mm × 400mm in structural-wall frame buildings. Beam sizes are 300mm × 400mm and structural wall sizes are 400mm × 400mm. Slabs are 150mm thick. Dimensions of all structural elements are uniform throughout the height of building. The materials are M30 grade concrete and Fe 415 steel. Beam-column joints are rigid. The effect is ignored of presence of masonry infill walls. The gross cross-section properties are considered, and not cracked properties, because this study focuses on initial proportioning of buildings in plan. The effect of masonry infill walls is not considered.

Equations (16) and (17) give only one value of τ for AMs of *Set S* for *all storeys* (if all member properties are same) and different τ values for AMs of *Set M* at each storey (even if all member properties are same) owing to absence of assumptions made in AMs of *Set S*. To account for these variations, modification factor is proposed when simple models are used. Hence, mean value is used for validation of τ of different storeys obtained from AMs of *Set M*. τ at each storey based on AM4 is validated by results of AM5, and used for identifying vertical irregularity in buildings.

Commercial software ETABS is used to perform structural analysis of the buildings. Rectangular walls are modelled using 2D shell elements and flanged-wall sections (*e.g.*, *angle and hollow core structural walls*) using frame element. The structural wall plan density SWPD is calculated separately along X- and Y- directions (*i.e.*, SWPD_X and SWPD_Y); it varies from 0.81 to 4.89% of plan area (Table 2). Rigid end zones are not modelled in frame elements. Slabs are considered rigid in their own plane. Only self-weight is considered of structural elements; additional gravity and lateral loads are ignored. τ ($=r_m/r_{K\theta}$) is estimated using the five analytical methods and verified through (T_{θ}/T) from 3D Modal Analysis of the buildings using ETABS software [14]. T_{θ} and T are estimated from predominant rotational and translational modes of the building using 3D MA; results are tabulated in Table 2. The results from Table 2 corresponding to 3D MA may not match

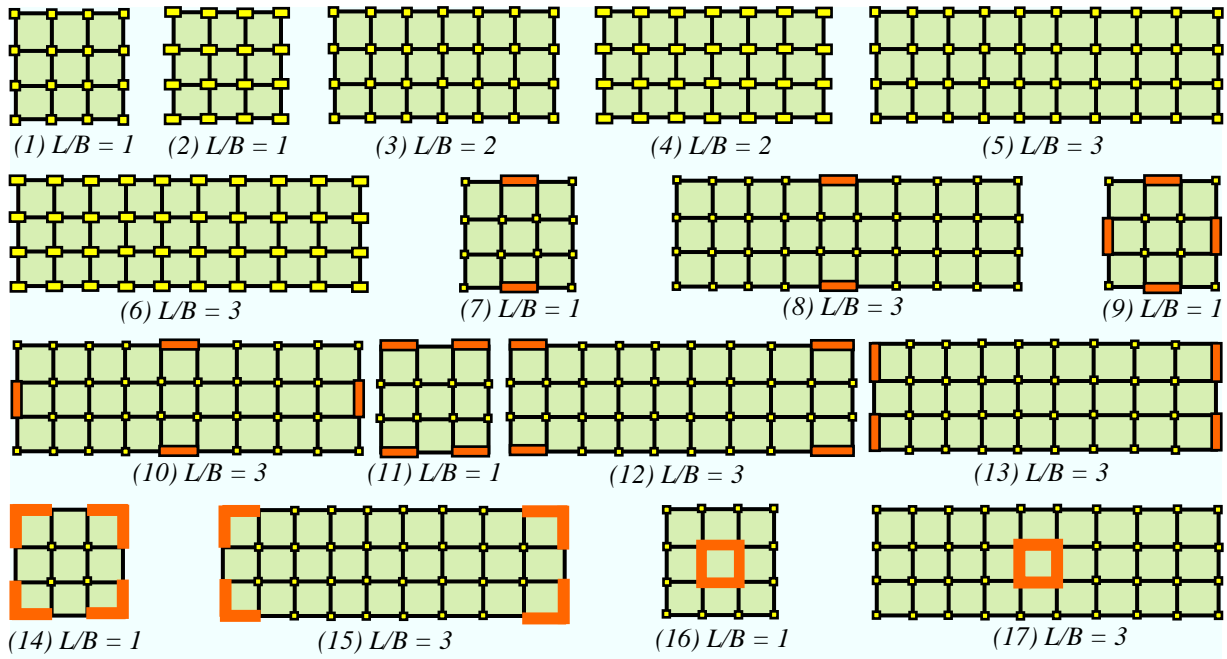


Figure 5: Spectrum of building configurations considered in this study.

Table 2: Estimates of τ using proposed AMs and 3D modal analyses.

BC	SWPD _x (%)	SWPD _y (%)	AM1		AM2		AM3		Modal Analysis				3D MA ($\tau = T_0/T$)	
									AM4		AM5			
			τ_x	τ_y	τ_x	τ_y	τ_x	τ_y	τ_x	τ_y	τ_x	τ_y	τ_x	τ_y
1	0.00	0.00	0.91	0.91	0.85	0.85	0.83	0.83	0.83	0.83	0.87	0.87	0.85	0.85
2	0.00	0.00	1.08	0.66	0.95	0.68	0.92	0.66	0.90	0.74	0.94	0.77	0.92	0.75
3	0.00	0.00	0.92	0.92	0.91	0.89	0.90	0.87	0.94	0.88	0.96	0.90	0.94	0.89
4	0.00	0.00	1.26	0.77	1.11	0.77	1.09	0.76	1.06	0.81	1.09	0.83	1.08	0.82
5	0.00	0.00	0.94	0.94	0.94	0.92	0.94	0.91	1.00	0.92	1.01	0.93	0.99	0.92
6	0.00	0.00	1.38	0.85	1.22	0.84	1.20	0.83	1.17	0.87	1.18	0.88	1.17	0.88
7	2.44	0.00	0.96	0.23	0.96	0.19	0.95	0.25	0.84	0.48	0.84	0.48	0.84	0.47
8	0.81	0.00	1.67	0.57	1.68	0.50	1.53	0.62	1.15	0.81	1.15	0.81	1.18	0.78
9	2.44	2.44	0.70	0.70	0.69	0.69	0.70	0.70	0.68	0.68	0.70	0.70	0.68	0.68
10	0.81	0.81	0.65	0.65	0.64	0.64	0.66	0.65	0.79	0.75	0.79	0.75	0.78	0.74
11	4.89	0.00	1.02	0.20	1.02	0.16	1.01	0.21	0.91	0.42	0.93	0.43	0.91	0.44
12	1.63	0.00	1.73	0.48	1.83	0.42	1.69	0.54	1.26	0.82	1.28	0.83	1.27	0.77
13	0.00	1.63	0.17	0.70	0.14	0.70	0.20	0.71	0.50	0.78	0.51	0.78	0.50	0.77
14	4.89	4.89	0.92	0.92	0.92	0.92	0.91	0.91	0.87	0.87	0.91	0.91	0.87	0.87
15	1.63	1.63	0.75	0.75	0.75	0.75	0.76	0.75	0.84	0.82	0.83	0.81	0.83	0.81
16	2.44	2.44	1.71	1.71	1.10	1.10	0.59	0.59	0.42	0.42	0.46	0.46	0.44	0.44
17	0.81	0.81	2.54	2.54	2.08	2.08	1.19	1.18	0.94	0.91	0.96	0.93	0.99	0.96

the same building results using SAP 2000 (*i.e.*, 3D MA results of Table 3 from literature, [13]), because rigid diaphragm constraints are not applied to same building models while using SAP 2000. The effects of various parameters influencing torsional flexibility in buildings are identified (using Figure 5 and Table 2), and the salient observations summarised in Table 3.

Figure 6 shows ratio of τ_N estimated from 3D MA and different analytical methods; Figures 6(a) and 6(b) show results without

and with including modification factor for *Set S*, respectively. The *Analytical Methods* are able to estimate the *3D Modal Analysis Responses* of RC moment frame and RC structural wall dominant buildings. *Set S* does not predict well in buildings with structural walls along one direction (*e.g.*, as in cases 7, 8, 11, 12 and 13) and in buildings with structural wall core at the center (*e.g.*, as in cases 16 and 17) (Figure 6(a)). It is due to the dominant interaction between the frames and structural walls due to fewer structural walls in one direction and stiff core at

Table 3: Effect of parameters influencing torsional flexibility in buildings on design.

S.No.	Structural Property	Influencing Parameters	Inference for Design
1	Radius of gyration r_m of rotational mass	(i) <i>Plan aspect ratio (L/B) of Buildings</i> For same sizes and shapes of structural elements, as L/B is varied from 1 to 3, torsional mode shifts from third mode to second mode (e.g., as in cases 2 and 6)	Avoid buildings with large L/B
2	Radius of gyration $r_{k\theta}$ of twisting stiffness	(i) <i>Size and shape of vertical elements</i> For a given L/B, as shapes of cross-sections is changed from square to rectangle, torsional mode shifts from third mode to second mode (e.g., as in cases 1 to 6) (ii) <i>Orientation of vertical walls along one plan direction of the building</i> (a) When structural walls are oriented along longitudinal plan direction (e.g., as in cases 7, 8, 11 and 12) with L/B changing from 1 to 3, torsional mode shifts from third mode to first mode and building becomes torsionally flexible ($\tau > 1$) (b) When structural walls are oriented along transverse plan direction (e.g., as in case 13), building becomes torsionally stiff; and (c) τ by different analytical methods AM1-AM5 varies drastically in the direction perpendicular to that of the wall. Therefore, when estimating r_m , contribution is ignored of these elements' lumped masses in I^M along its major direction. Thus, the mean τ values (using AM4 and AM5) are in good agreement with 3D MA (i.e., T_{θ}/T). (iii) <i>Orientation of structural walls along two plan directions of the building</i> When structural walls are located along the periphery (e.g., as in cases 9, 10, 14 and 15), buildings become torsionally stiff ($\tau < 1$) even when L/B changes from 1 to 3. (iv) <i>Location of stiff structural wall core in structural wall-frame buildings</i> When structural core wall is at the center (e.g., as in cases 16 and 17), buildings are torsionally flexible ($\tau > 1$), and the effect gets worse with increase in L/B (v) <i>Height of the building</i> Variation of τ_i at storey i along the height of building (estimated using AM4 and AM5) showed that: (a) Torsionally stiff buildings become torsionally flexible (e.g., as in cases 5, 8, 12) with walls in one direction with large L/B (=3); sometimes, torsionally stiff buildings become torsionally flexible, when walls are oriented in one direction when L/B is small (=1), or limited walls are present along both directions when L/B is large (=3); and (b) Torsionally flexible become torsionally stiff in a few cases (e.g., as in cases 16 and 17) because the presence of stiff structural wall core changes translationally stiff-torsionally flexible building to translationally flexible-torsionally stiff	Provide square shaped vertical elements, especially along the periphery (a) Avoid buildings with large L/B; (b) Provide structural walls to torsionally stiffen the buildings; and (c) Provide structural wall in both directions, especially along the periphery Provide structural wall in both directions, and especially at periphery Provide structural wall along the periphery, rather than confining them at the center Provide at least a minimum area of walls along both plan directions;

center. It is accounted for directly using 3D MA, but the simplified analytical methods do not consider these effects as it considers only distribution of mass and stiffness in plan. Therefore, modification factor is used in these analytical methods to get results like that of AM4 (Figure 6(b)). Mean values of τ based on Set M show almost similar result as 3D MA (Figure 6, Table 2).

Analytical Method AM4 can be employed rather than AM5, because AM5 requires estimation of storey lateral forces and torsional moments, which is cumbersome. The average error in results of AM4 and AM5 with respect to those of 3D MA for

all floors of all building configurations studied (Table 4) are minimal. Also, only in a few cases, there are variations (e.g., ~7.6% for case 7) observed at top storey of these buildings; otherwise, the error at each storey is small or uniform along the height. Using Set S, the accuracy is found to be good in almost regular buildings having uniform mass and stiffness distribution (~0 to 18%). In other buildings, the error is larger (Table 4). In all, the observations remain same by all five analytical methods in single- and multi-storey buildings, though there is variation in their magnitude. Even then, analytical methods in Set S are simple and effective to identify torsional flexibility in buildings

without any software-based structural analysis. AM4 closely predicts 3D MA response as it considers the deformed configuration of building to consider the stiffness variation along its height. These approaches can be adopted in buildings

with complex plan geometries having rigid diaphragms. Hence, code provision should include this parameter τ in defining both torsional irregularity ($\tau > 1$, as defined in *Indian code*, IS 1893(1) [15]) and vertical irregularity in buildings.

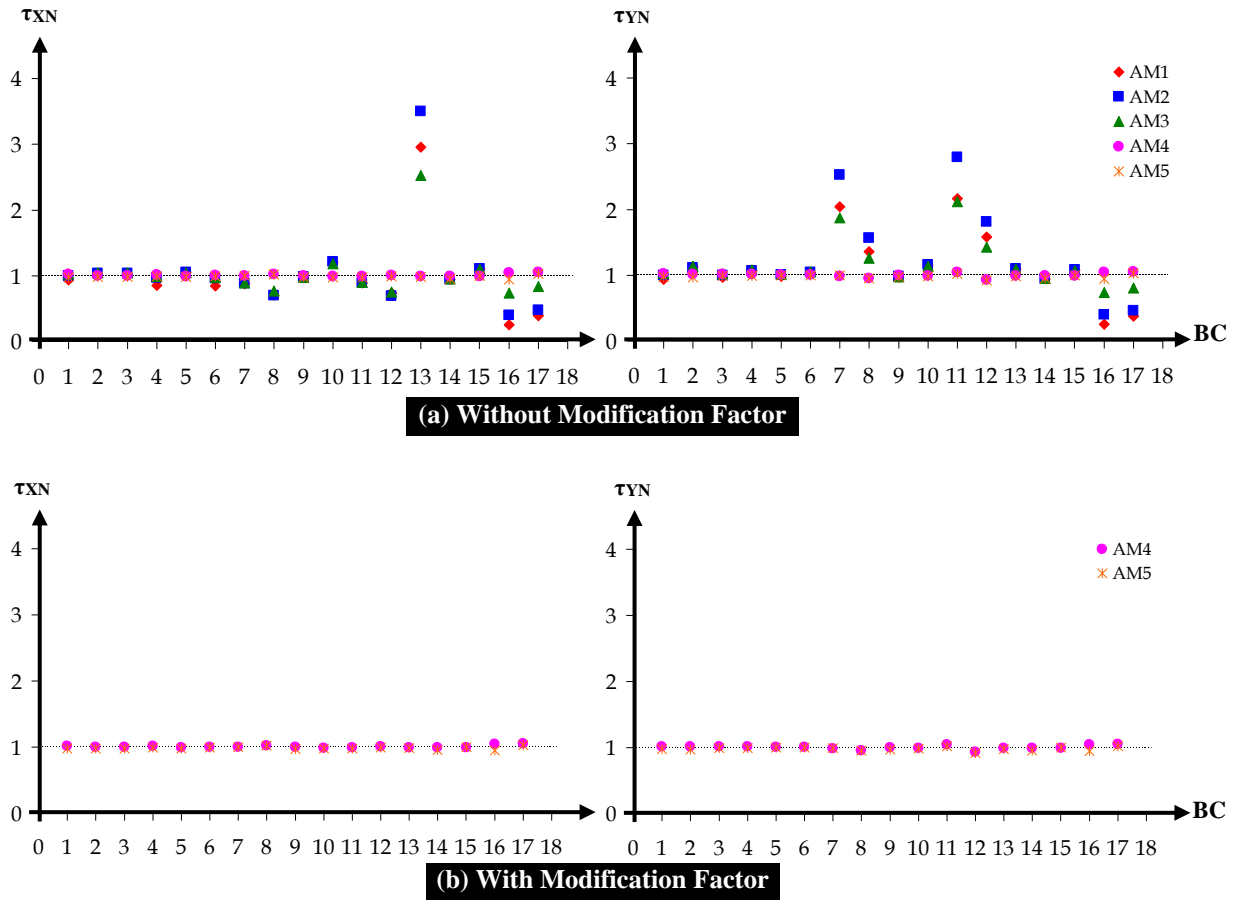


Figure 6: Ratio $\tau_N (= \tau_{3D MA} / \tau_{AM})$ of results from 3D MA and: (a) five analytical methods (AM1–AM5) along X- and Y-directions without including modification factors, and (b) two analytical methods (AM4–AM5) along X- and Y-directions including the modification factors for Set S.

Table 4: Errors in results from Approximate Methods compared to those from 3D MA, averaged over all floors for all building configurations studied.

S.No.	Type of Buildings	Average % error of AMs (r_{mi}/r_{K0i}) compared to 3D MA (T_{θ}/T)				
		Single-Storey Models			Multi-Storey Models	
		AM1	AM2	AM3	AM4	AM5
1	Moment Frame Building	1.3 – 17.9	0.1 – 9.9	0.7 – 11.8	0 – 2.6	0.2 – 3.3
2	Structural Wall-Frame Buildings					
	(a) Structural walls oriented along one direction	8.6 – 66.2	8.8 – 71.5	8.0 – 60.4	0.1 – 7.3	0.1 – 8.7
	(b) Structural walls oriented along both directions	3.6 – 16.9	2.1 – 17.8	2.5 – 15.7	0.3 – 1.2	0.1 – 5.0
	(c) Structural walls in the core only	156.8 – 292.6	110.5 – 152.4	20.0 – 35.9	4.5 – 5.1	2.8 – 5.7

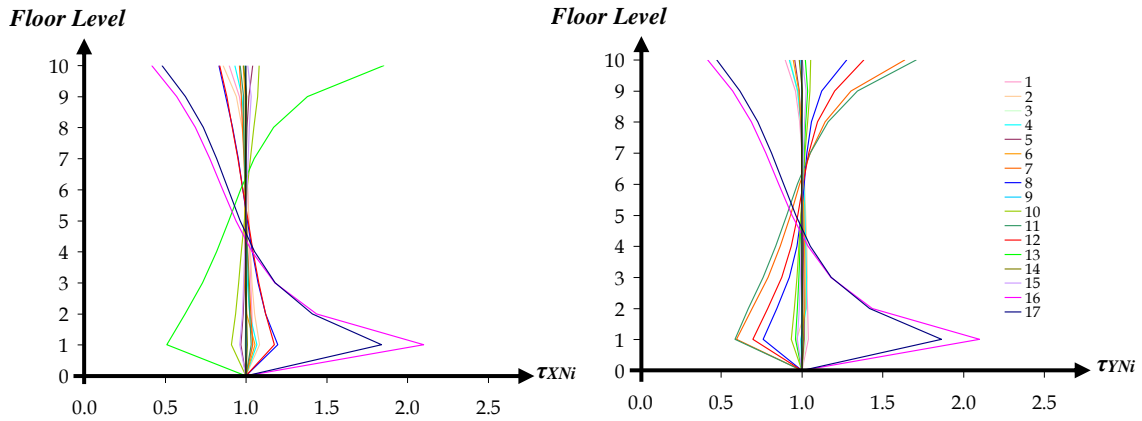


Figure 7: Normalised τ_{Ni} ($=\tau_i/\tau_{i,avg}$) estimated from the ratio τ_i at storey i and $\tau_{i,avg}$ of AM4 along X- and Y-directions, to check vertical regularity in buildings along their height.

Figure 7 shows the normalised τ_{Ni} ($=\tau_i/\tau_{i,avg}$) estimated as a ratio of τ_i at storey i and $\tau_{i,avg}$ of each buildings calculated using AM4 to check the vertical regularity of building along its height. Vertically regular buildings show uniform distribution of mass and stiffness along the height of buildings, and hence relatively uniform τ_i along the height; when τ_i is not relatively uniform along the height, building becomes vertically irregular. RC moment frame and RC structural wall buildings (having walls along both plan directions, e.g., as in cases 9, 10, 14 and 15) show almost uniform variation of τ_i along the height of building (though, some minor variations are noticed at base and roof levels of buildings, due to varying boundary conditions). But, variations are noticed in buildings (even with uniform mass and stiffness distribution along height) when: (i) structural walls are oriented along one direction, particularly in direction perpendicular to orientation of walls (e.g., as in cases 7, 8, 11, 12, and 13), (ii) structural wall core are symmetric along both directions and placed at the CM of the building in plan (e.g., as in cases 16 and 17), and (iii) sometimes, building mentioned in (i) and (ii) above show variations in both directions due to larger L/B ($=3$) (e.g., as in cases 8, 12, 17). It is solely identified based on distribution of mass and stiffness at each storey. Also, such buildings behave differently depending up on the interaction between frames and structural walls depending upon the quantity of structural walls and larger plan aspect ratio. On the whole, the proposed approach can be adopted to identify vertical irregularity in RC buildings with moment frames or with structural walls in both plan directions. Also, it is recommended to: (i) avoid buildings with large L/B , (ii) provide structural walls in both directions, and (iii) avoid confining structural walls at center.

Behaviour of Idealised Single Storey Models

A single-storey idealised 3-element model (Figure 8) is used to study the lateral-torsional behaviour of unsymmetrical buildings using 2 degrees of freedom (*one translation and one rotation*). It assumes rigid diaphragm with uniform mass distribution and the reference axis passes through the CM. Therefore, the building becomes unsymmetrical by varying the stiffness distribution of 3 elements and location of middle element; also, it becomes torsionally flexible by varying the stiffness distribution of middle element and plan aspect ratio L/B . In all, 35 idealised 3-element configurations are considered by varying plan aspect from 1/3 to 3 (as the L/B is restricted to 3 [15]) and location of middle element. The lateral-torsional response in building is influenced by two critical parameters namely torsional eccentricity e_K and natural period ratio τ . The normalised torsional eccentricity (e_K/B , B is the building lateral dimension) is varied from 0.0 to 0.40 and $\tau = 0.61$ to 2.22. Using

the 3-element model with $L/B \geq 2$, τ always remains greater than 1. Torsional flexibility of the buildings increases with increase in stiffness distribution of middle element and L/B . Hence, code provisions placed an upper limit on $L/B = 3$. The extreme element response amplification increases in buildings with larger e_K/B and $\tau > 1$. Hence, in this study, design limits are proposed based on critical parameters; the overall observations are validated through linear and nonlinear dynamic analysis of multistorey buildings [1]. Also, simple methods to estimate torsional eccentricity using single- and multi-storey buildings are discussed elsewhere [16].

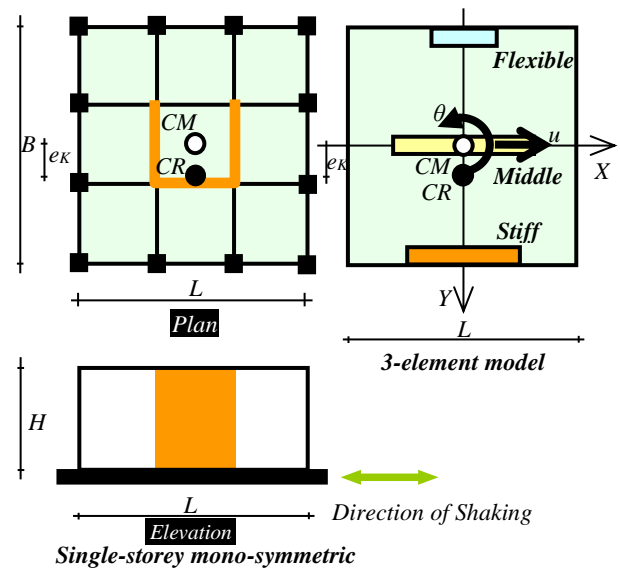


Figure 8: One storey building and idealised 3-element model [1].

Behaviour of Torsionally Flexible Multistorey Buildings

Six storey torsionally flexible buildings (having response reduction factor $R = 3$ and 5) are used to demonstrate their vulnerability under earthquake shaking (Figure 9). The building has 4m storey height and 6m bay lengths having 30m overall plan dimensions in each direction ($L/B=1$). The slab and infill wall thicknesses are taken as 150mm and 250mm, respectively. Size of beams, columns and structural walls are taken as 300mm \times 400mm, 500mm \times 500mm and 6000mm \times 300mm, respectively. The $SWPD_x$ and $SWPD_y$ are calculated as 0.42% of total plan area. The grades of concrete and steel are M30 and Fe 415. Unit weight of infill wall is taken as 20 kN/m³. The floor finish, live load on all floors and roof is taken as 1 kN/m²,

3 kN/m² and 1.5 kN/m², respectively. Also, the buildings are assumed to be in seismic zone V and hard rock (Type I) soil. Importance factor is taken as 1. Earthquake induced lateral loads are calculated using IS 1893(1), and structural analysis is conducted using ETABS software. Effective stiffness for beams and columns is taken as 0.35 and 0.7. Using Modal Analysis, the translational and torsional natural periods are given by $T_X = T_Y = 0.593s$ and $T_\theta = 0.807s$, and $\tau_x = \tau_y = 1.36 (>1)$, first mode of the building is torsional). The mass participation in translational and torsional modes is found to be 70.6% and 85.6%. Building with R=3 is designed, and detailed using IS 456 [17], and R=5 using IS 456 and IS 13920 [18], respectively. But, the shear failure is avoided in both the buildings.

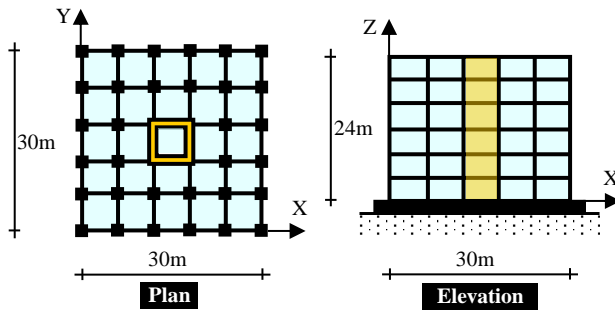


Figure 9: Torsionally flexible building with structural wall core at center.

Nonlinear static (NLPoA) and nonlinear time history (NLTHA) analyses are conducted using Perform 3D software [19]. 30 far-field strong ground motions (of magnitudes M6.3 to M7.3 having epicentral distances of 20 km to 50 km [20,21]) are used in principal X-direction (unidirectional). These ground motions are scaled (by spectral scaling) such that of pseudo-acceleration response matches the design acceleration spectrum value at fundamental natural period of the building. Both buildings have same natural period, but have different R values (without and with ductile detailing, R= 3 and 5). It helps to understand the behaviour of buildings with same lateral stiffness and strength under same intensity of ground motions. Confined concrete properties [22] are estimated for core concrete and without confinement for cover concrete (strain limit of 0.0035). Strain in steel is limited to 0.05 to account for cyclic load effects [23]. Point plasticity is considered in beams with idealised bilinear moment-curvature curve (considering yielding of steel and crushing of core concrete [24]). Whereas columns and structural walls are modelled using fibres of concrete and steels (idealised as bilinear curve). The collapse in building is decided based on crushing of extreme fibre of confined core concrete in column (reaching limiting strain in bending compression). The effect of P-delta is not considered. All structural elements are assumed to follow kinematic hysteresis rules on elastic-plastic backbone curve without stiffness and strength deterioration. The validation of building models in Perform 3D is carried out by modelling elastic and inelastic properties of building archetype ID 1010 [25]. Almost initial lateral stiffness and peak strength matches Perform 3D result with around 12.7% variation in failure strain. Also, using elastic and inelastic properties of present study, an experimentally tested building model [26] is validated in Perform 3D. Initial lateral stiffness and failure strain almost matches the Perform 3D results and peak strength shows ~6.4% variation.

Using code based lateral load distribution, capacity curves (lateral strength V normalised with seismic weight) are calculated for both buildings. The capacity spectrum method is used to estimate the performance point for the demand spectrum corresponding to 0.36g (Zone V) [27]. Using 30 ground

motions, maximum inelastic drift is estimated ($\mu + \sigma$, where μ is mean and σ , standard deviation) using nonlinear time history analysis. The inelastic drift obtained from a few critical ground motions (GM 01: Cape Mendocino – Fortuna, GM 02: Coalinga – Fault Zone 10, GM 03: Coalinga – Gold Hill 3E, GM 04: Landers – Pal Springs Airport, GM 05: San Fernando – Lake Hughes, GM 06: San Fernando – Palmdale Fire Station, GM 07: Kobe – OSAJ) evidences the maximum inelastic drift ranges being nearer to performance point (Figure 10). Building with R=5 has good energy dissipation capacity than R=3. Both the buildings show similar lateral strength and stiffness but different deformation capacity under NLPoA; but the inelastic drift pattern remains same under nonlinear time history analysis (Figures 10 and 11). In overall, structural behaviour starts with yielding of beams, columns and structural walls; then, beams have failed by reaching its ultimate moment capacity and eventually the structure fails with crushing of core concrete in columns. The damages in structural elements are calculated when it reaches $\geq 80\%$ yield strain or yield curvature and $\geq 80\%$ ultimate strain or ultimate curvature. The damage mechanisms at yielding and ultimate failure of structural elements are shown in Figure 12.

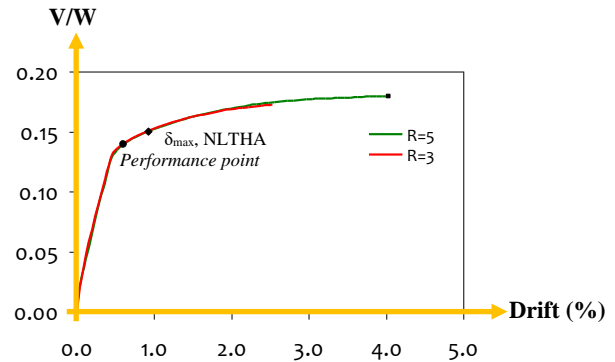


Figure 10: Comparison of capacity curves of buildings with R = 3 and 5.

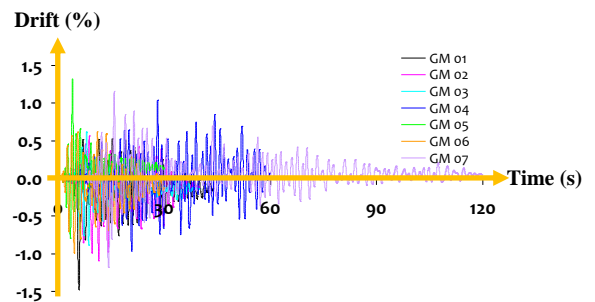


Figure 11: Inelastic drift at roof top measured for a few different ground motions in buildings with R = 3 and 5.

The hysteresis behaviour of beam connected to structural wall at fifth storey (which is failed) and corner column at ground storey are obtained under a few ground motions (Figure 13). Though both the buildings show almost similar response at structure level, variation in response is noticed under element behaviour. Also, damages are more in buildings with R=3 than R=5 (Figure 12 and 13). Building with R=3 shows ~14 to 57% of beams have damaged and ~51% of beams failed completely by reaches its ultimate curvature capacity; but only minor damages are observed in columns (~21%). On the other hand, in building with R=5, ~16 to 57% of beams have damaged and ~5% of beams failed completely by reaches its ultimate curvature capacity; but only minor damages are observed in columns (~18%). In both the buildings, structural walls have

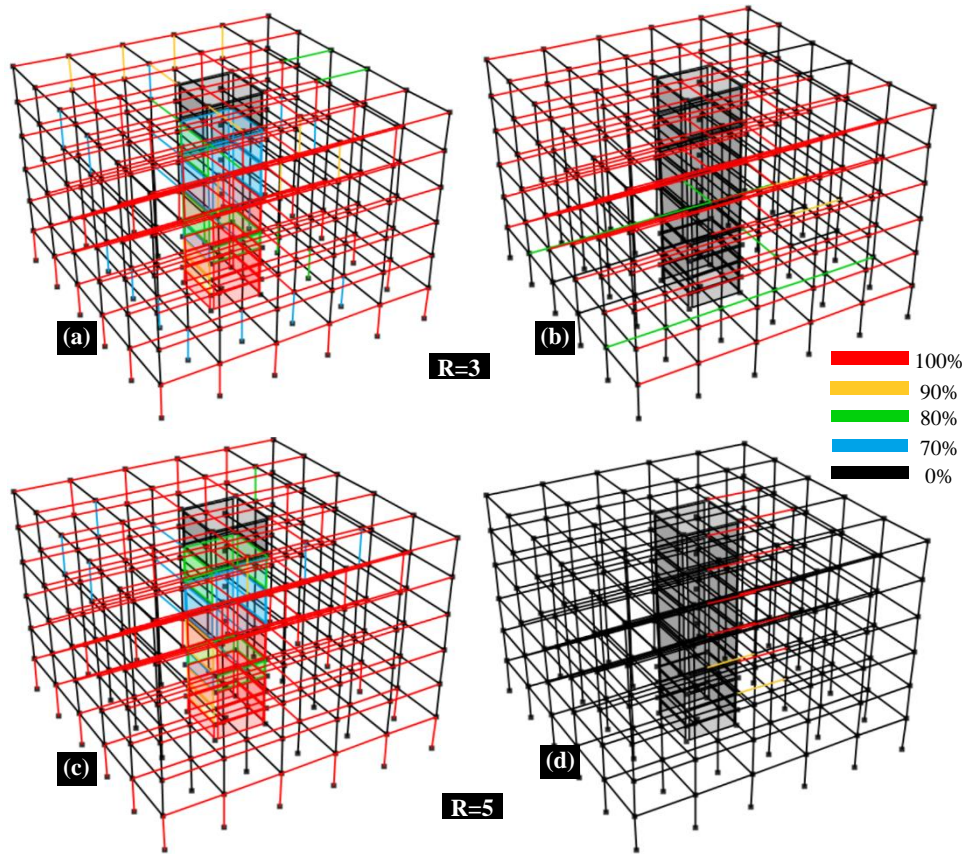


Figure 12: Comparison of damages observed during yielding and ultimate failure in structural elements under Coalinga Earthquake (GM 02): (a) and (b) yielding and ultimate failure for building with $R=3$, (c) and (d) yielding and ultimate failure for building with $R=5$.

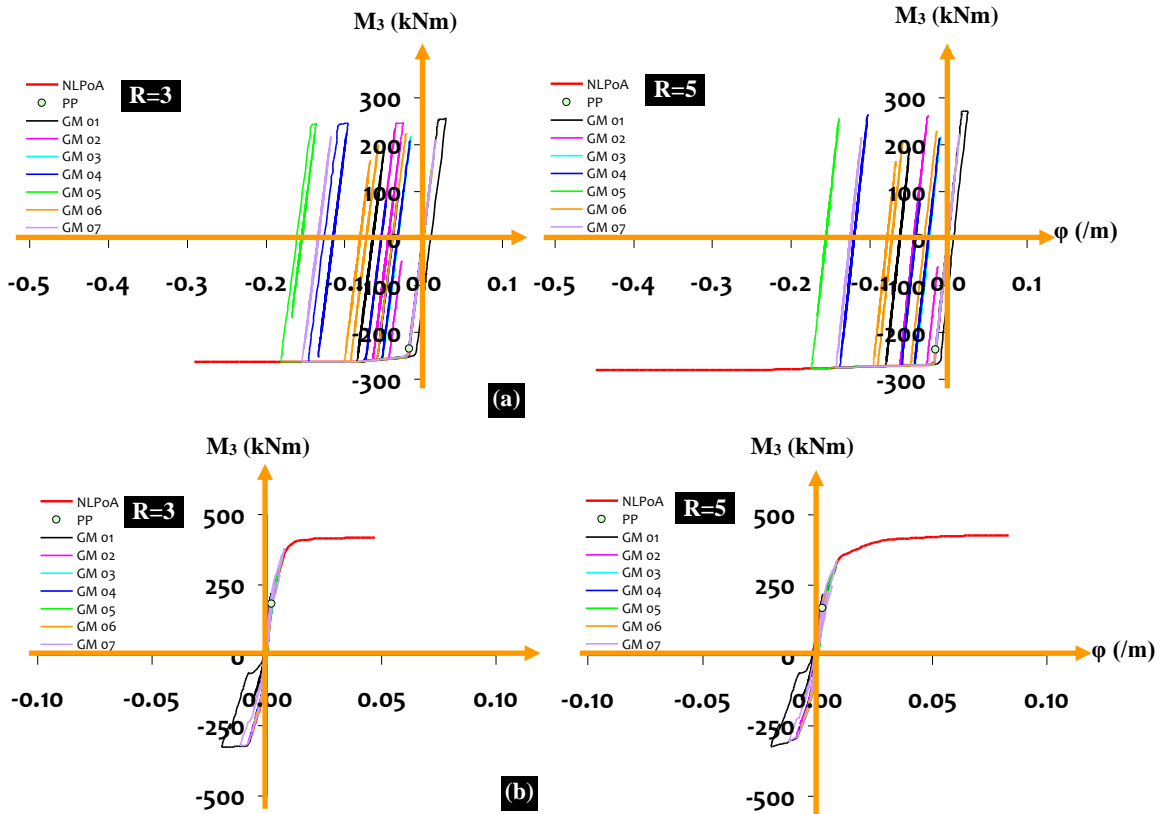


Figure 13: Monotonic and hysteretic behaviour of critical beams and columns under a few ground motions using moment curvature behaviour of (a) beams and (b) columns.

undergone only minor damages. But, usually the beams connected to structural walls always fail under design level shaking by losing the connection between the structural wall core and beams, even if $R = 5$. This evidences the failure in 2001 Bhuj earthquake, where the lift core stood alone with rest of the buildings failed losing their gravity load carrying capacity (Figure 1(a)). Thus, it is advisable to avoid torsionally flexible buildings.

Effect of Angle of Shaking

Based on the selected seven critical ground motions, the torsional behaviour of these buildings is studied by varying the angle of excitation of ground motion GM_θ ($= 0^\circ, 30^\circ, 45^\circ$ and

60°) in one direction with respect to X. The inelastic drift along X direction increases when $GM_\theta = 0^\circ$ to 30° and it decreases from 30° to 60° . Because as the GM_θ increases, from 30° to 60° , the component of shaking is more in Y direction than X direction; conversely, inelastic drift responses decreases when $GM_\theta = 0^\circ$ to 30° and increases from 30° to 60° in Y-direction. In a few cases, the level of damages increasing with increase in GM_θ , causing permanent deformations (e.g., drift response under GM 07, where the responses are shifted from the X-axis) (Figure 14). Additionally, equal and opposite rotational behaviour is noticed when GM_θ is 30° or 60° , with no rotational components for 0° or 45° . Also the magnitude of rotation increases with yielding and becomes almost constant after complete yielding (e.g., $\theta=0.00033^\circ$ for GM 07) (Figure 15).

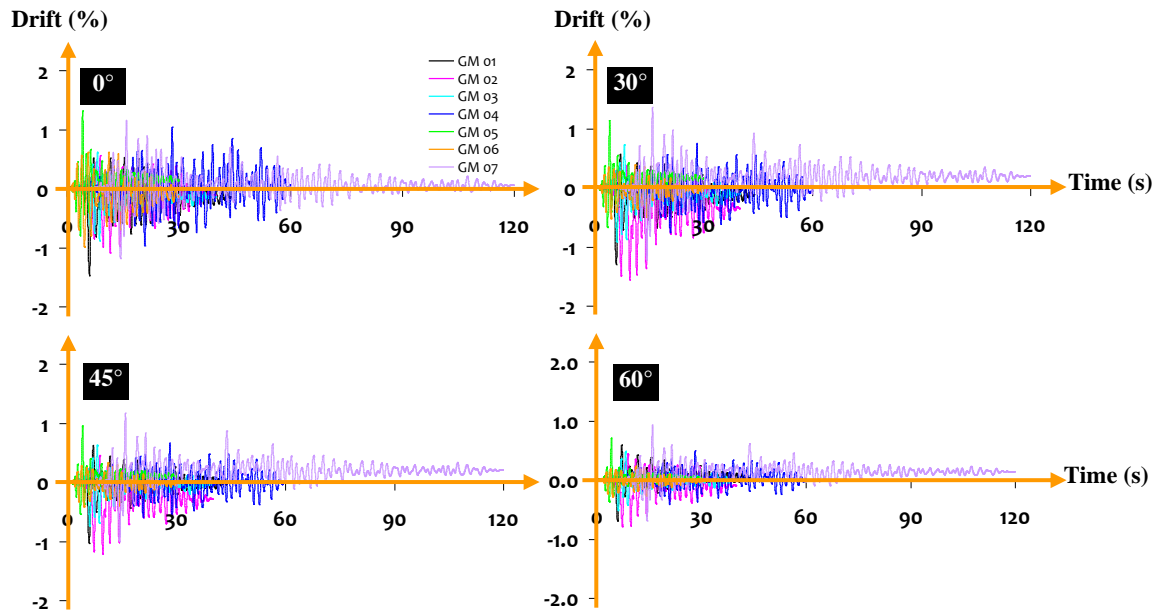


Figure 14: Inelastic drift at roof top measured for a few different ground motions in buildings with $R=5$ for $GM_\theta = 0^\circ, 30^\circ, 45^\circ$ and 60° .

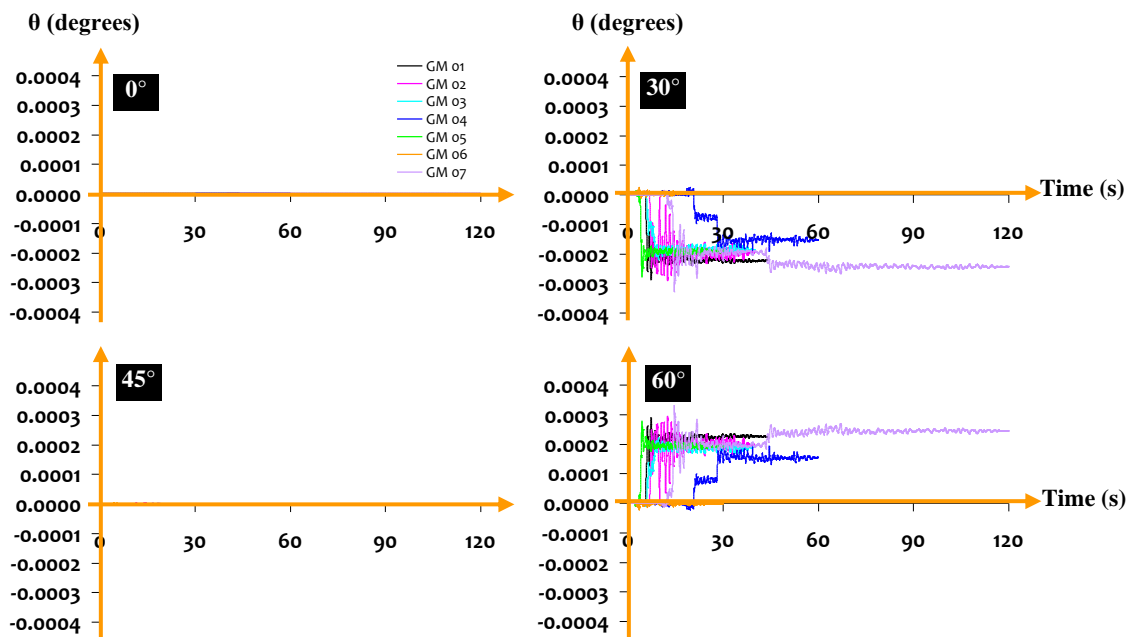


Figure 15: Inelastic rotational response at roof top measured for a few different ground motions in buildings with $R=5$ for $GM_\theta = 0^\circ, 30^\circ, 45^\circ$ and 60° .

Though the magnitude of rotation is lesser, it in turn results in more drift in X direction for $GM_\theta = 30^\circ$ than 0° (e.g., inelastic drift increases from 1.21% to 1.36% for GM 07). These deformations will be amplified more with the presence of torsional eccentricity in torsionally flexible buildings (e.g., C shaped lift core showed poor energy dissipation capacity and caused huge damage in unidirectional shaking i.e., ~30-50% beams have ultimately failed, and many columns or structural walls are damaged sustaining more rotational response. Thus, the torsionally flexible building becomes more critical due to the presence of torsional eccentricity). Hence, the building codes must place upper limit on these critical parameters [1].

Table 5 and Figure 16 demonstrate the damages in structural elements at yielding and ultimate limit state. The damages in beams and columns are almost doubled with change in the angle

of excitation (e.g., 52.4 – 57.1% to 73.5 – 100% for 0° to 45°). Also, similar level of damages is noticed when $GM_\theta = 30^\circ$, 45° , and 60° . Alternately, with change in GM_θ , structural walls showed more yielding and sometimes in a few cases, it has failed (e.g., building with $R=5$ under 30° , 45° and 60° under GM 02). Thus, it is mandatory to avoid torsionally flexible buildings (Table 5 and Figure 16). Figure 17 shows the hysteretic behaviour of columns (in both directions), beams and structural walls under GM 02. The level of inelastic action is more when $GM_\theta = 30^\circ$ in all structural elements. The inelastic behaviour is more in M_2 direction of the column for $GM_\theta = 60^\circ$ as the ground motion is almost inclined towards Y direction and as expected the magnitude of response is like M_3 direction for $GM_\theta = 30^\circ$. This level of damages may increase for bi-directional shaking.

Table 5: Damages in structural elements under varying angle of shaking GM_θ .

R	GM_θ	Beams (%)		Columns (%)	Structural Walls (%)	
		Yield	Ultimate	Yield	Yield	Ultimate
3	0°	52.4 – 57.1	25.6 – 50.6	9.4 – 21.9	45.8 – 66.7	–
	30°	58.9 – 100.0	1.2 – 63.1	11.5 – 35.4	50.0 – 58.3	–
	45°	73.5 – 100.0	1.2 – 79.8	14.1 – 35.4	50.0 – 50.0	–
	60°	58.9 – 100.0	1.2 – 61.3	11.5 – 35.4	50.0 – 54.2	–
5	0°	51.5 – 57.1	1.2 – 5.4	7.3 – 18.2	45.8 – 70.8	–
	30°	59.8 – 98.9	0.0 – 7.7	12.0 – 33.9	50.0 – 66.7	0.0 – 4.2
	45°	73.2 – 100.0	0.0 – 6.0	14.6 – 34.4	50.0 – 66.7	0.0 – 8.3
	60°	59.8 – 98.8	0.0 – 9.2	12.0 – 33.9	50.0 – 66.7	0.0 – 4.2

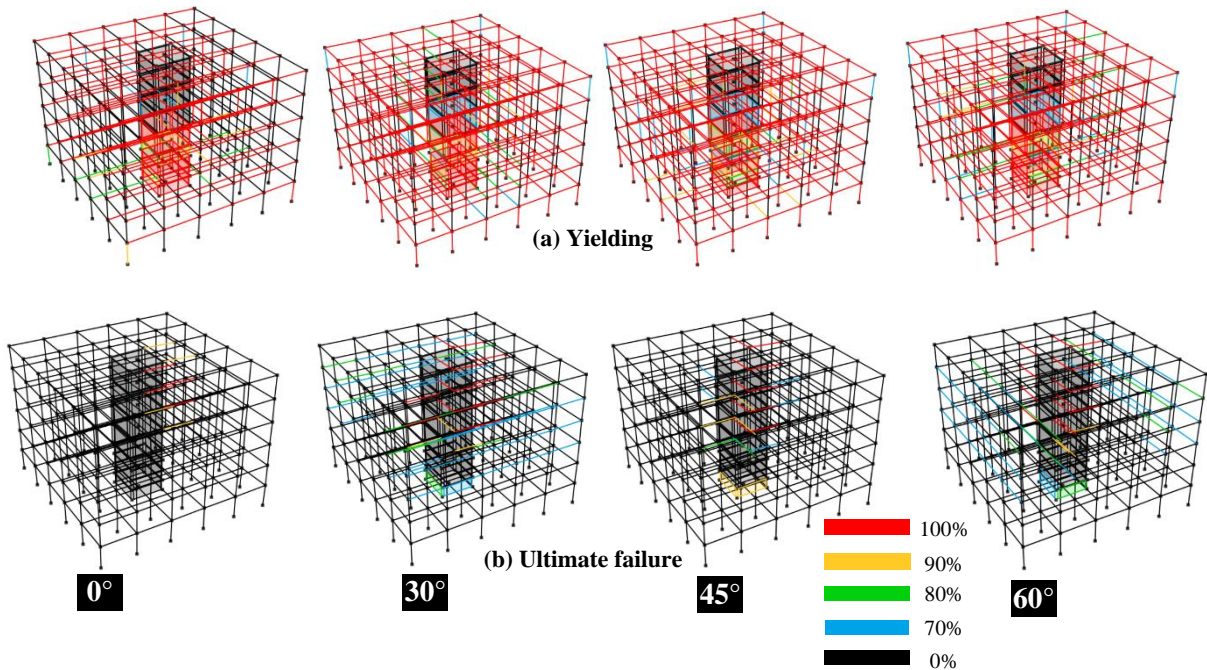


Figure 16: Comparison of damages observed during (a) yielding and (b) ultimate failure in structural elements under Coalinga Earthquake (GM 02) in buildings with $R= 5$ for $GM_\theta = 0^\circ, 30^\circ, 45^\circ$ and 60° .

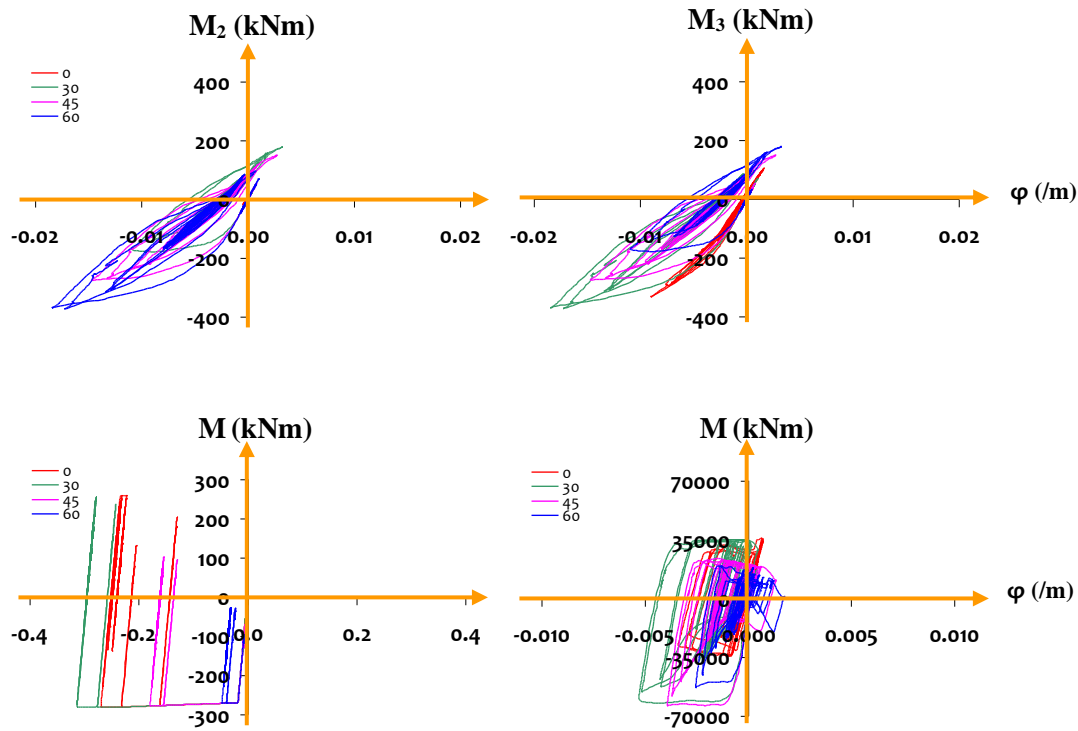


Figure 17: Hysteretic moment curvature behaviour of (a) columns in both directions (b) beams, and (c) structural walls under Coalinga Earthquake (GM 02) in buildings with $R= 5$ for $GM_{\theta} = 0^{\circ}, 30^{\circ}, 45^{\circ}$ and 60° .

CONCLUSIONS

Building code provisions are becoming explicit to avoid *torsionally flexible buildings* ($\tau > 1$, where $\tau = r_m/r_{K\theta}$ or T_{θ}/T). In general, these requirements meant for plan and elevation regular buildings with relatively small eccentricity. *Simple Methods* using *single storey models* (with vertical elements in considered storey is fixed at their two ends, or with rotational flexibility of beams connecting at the top and bottom ends of the vertical element) can identify such buildings during initial proportioning, before conducting the detailed structural analysis. Here, hand-calculations can be performed to identify the *torsionally flexible buildings*. This study also considered *Detailed Methods* using *multi-storey models* of buildings, which require results of 3D modal analysis of buildings to identify the *torsionally flexible buildings*. The simple methods analytical methods are validated with *3D Modal Analysis*. Also, parameters influencing torsional flexibility are identified. Finally, the poor performance of a torsionally flexible building is demonstrated using nonlinear static and dynamic analyses, and by varying the angle of shaking.

The following are the salient conclusions drawn from this study (to control the worst effects of buildings becoming torsionally flexible):

1. *Simple Method* is sufficient to identify analytically the torsional flexibility in *RC moment frame buildings* and *RC structural wall buildings*;
2. *Detailed Method* (3D Modal Analysis) is required for: (a) *buildings with structural walls oriented along one direction only*, (b) *buildings with structural wall cores* to capture torsional flexibility in buildings, and (c) buildings with complex plan geometries and rigid diaphragms. Alternately, the simple methods can be used with modification factors suggested, but this will required significant effort to calibrate the factors; and
3. Recommendations for design are:
 - (a) Avoid buildings with large plan aspect ratio $L/B > 2$;

- (b) Provide at least a minimum percentage of structural walls in each plan direction, especially along the periphery of buildings; a detailed study is required for determining this minimum value; and
- (c) Use τ to identify vertical irregularity in buildings.

REFERENCES

- 1 Tamizharasi G, Prasad AM and Murty CVR (2021). "Lateral-torsional seismic behaviour of plan unsymmetric buildings". *Earthquakes and Structures*, Techno Press, **20**(3): 239-260. <https://doi.org/10.12989/eas.2021.20.3.239>
- 2 Omidvar B, Sadeghian A and Nojavan M (2014). "The role of architectural considerations in seismic performance of buildings: A case study in Iran". *Journal of Civil Engineering and Architecture*, **8**(3): 268-275. <https://pdfs.semanticscholar.org/8233/8386f429ce4925dbbe3efc2ab3ed70505f79.pdf>
- 3 Das PK, Dutta SC and Datta TK (2021). "Seismic behavior of plan and vertically irregular structures: State of art and future challenges". *Natural Hazards Review*, **22**(2): 1-17. [https://doi.org/10.1061/\(ASCE\)NH.1527-6996.0000440](https://doi.org/10.1061/(ASCE)NH.1527-6996.0000440)
- 4 Fierro EA (2007). "Learning from Earthquakes: The Pisco, Peru, Earthquake of August 15, 2007". Earthquake Engineering Research Institute Special Earthquake Report, **9**(6), 1-12. https://www.eeri.org/lfe/pdf/peru_pisco_eeri_preliminary_reconnaissance.pdf
- 5 Murty CVR, Brzev S, Faison H, Comartin CD and Irfanoglu A (2006). "At Risk: The Seismic Performance of Reinforced Concrete Frame Buildings with Masonry Infill Walls". Publication No. WHE-03, Earthquake Engineering Research Institute, Oakland, California, 1-70. https://www.world-housing.net/wp-content/uploads/2011/05/RCFrame_Tutorial_English_Murty.pdf

- 6 Trujilo NB (1985). *Mexico City Earthquake Summary and Lessons Learned*, BAE, Penn State, 2002.
- 7 Tabatabaei R (2011). "Torsional Vibration of Eccentric Building Systems". *Recent Advances in Vibrations Analysis*, Intech, 169-192. <https://doi.org/10.5772/21997>
- 8 Mehana MS, Mohamed O and Isam F (2019). "Torsional behaviour of irregular buildings with single eccentricity". *In IOP Conference Series: Materials Science and Engineering*, 603(5): 052028. <https://doi.org/10.1088/1757-899X/603/5/052028>
- 9 Raheem SEA, Ahmed MM, Ahmed MM and Abdel-shafy AG (2018). "Evaluation of plan configuration irregularity effects on seismic response demands of L-shaped MRF buildings". *Bulletin of Earthquake Engineering*, **16**(9): 3845-3869. <https://doi.org/10.1007/s10518-018-0319-7>
- 10 Botis MF and Cerbu C (2020). "A method for reducing the overall torsion for reinforced concrete multi-storey irregular structures". *Applied Sciences*, **10**(16): 1-25. <https://doi.org/10.3390/app10165555>
- 11 Vijayanarayanan AR, Goswami R and Murty CVR (2017). "Estimation of storey stiffness in multi-storey buildings". *Proceedings of the Sixteenth World Conference on Earthquake Engineering, 16WCEE*, Paper No. 415, Santiago, Chile. <https://www.wcee.nicee.org/wcee/article/16WCEE/WCEE2017-415.pdf>
- 12 Liu R, Chen R, Jiang Y and Liu W (2012). "Lumped-mass stick modeling of building structures with mixed wall-column components". *Proceedings of the Fifteenth World Conference on Earthquake Engineering, 15WCEE*, Lisbon, Portugal. https://www.iitk.ac.in/nicee/wcee/article/WCEE2012_342_1.pdf
- 13 Tamizharasi G, Prasad AM and Murty CVR (2020). "A simple method to identify torsional flexibility in buildings without performing detailed structural analysis". *Proceedings of the Seventeenth World Conference on Earthquake Engineering, 17WCEE*, Paper No.:2c-0235, Sendai, Japan, 1-12. <https://wcee.nicee.org/wcee/article/17WCEE/2c-0235.pdf>
- 14 ETABS (2020). *Analysis and Design of Building Systems*, Version 18.1.1, Computers and Structures Inc. (CSI), USA.
- 15 Bureau of Indian Standards (2016). "Indian Standard Criteria for Earthquake Resistant Design of Structures, Part 1 General Provisions and Buildings". IS 1893(1), New Delhi, India.
- 16 Tamizharasi G and Murty CVR (2022). "Identifying torsional eccentricity in buildings without performing detailed structural analysis". *Earthquakes and Structures*, Techno Press, **23**(3): 283-295. <https://doi.org/10.12989/eas.2022.23.3.283>.
- 17 Bureau of Indian Standards (2000). "Indian Standard Code of Practice for Plain and Reinforced Concrete". IS 456, New Delhi, India.
- 18 Bureau of Indian Standards (2016). "Indian Standard Code of Practice for Ductile Detailing of Reinforced Concrete Structures Subjected to Seismic Forces". IS 13920, New Delhi, India.
- 19 Perform 3D (2021). *Nonlinear Analysis and Performance Assessment for 3D Structures*, Version 8, Computers & Structures Inc. (CSI), USA.
- 20 Huang YN, Whittaker AS, Luco N and Hamburger OR (2011). "Scaling earthquake ground motions for performance-based assessment of buildings". *ASCE Journal of Structural Engineering*, **137**(3): 311-321. [https://doi.org/10.1061/\(ASCE\)ST.1943-541X.0000155](https://doi.org/10.1061/(ASCE)ST.1943-541X.0000155).
- 21 Reyes JC, Riano AC, Kalkan E, Quintero OA and Arango CM (2014). "Assessment of spectrum matching procedure for nonlinear analysis of symmetric-and asymmetric-plan buildings". *Engineering Structures*, **72**: 171-181. <https://doi.org/10.1016/j.engstruct.2014.04.035>
- 22 Mander JB, Priestley MNJ and Park R (1988). "Theoretical stress-strain model for confined concrete". *ASCE Journal of Structural Engineering*, **114**(8): 1804-1826. [https://doi.org/10.1061/\(ASCE\)0733-9445\(1988\)114:8\(1804\)](https://doi.org/10.1061/(ASCE)0733-9445(1988)114:8(1804))
- 23 Federal Emergency Management Agency (2000). "FEMA 356: Prestandard and Commentary for the Seismic Rehabilitation of Buildings". Washington, D.C. <https://www.nehrp.gov/pdf/fema356.pdf>
- 24 Sunitha P, Goswami R and Murty CVR (2016). "Idealised bilinear moment-curvature curves of RC sections for pushover analysis of RC frame buildings". *Indian Concrete Journal*, **90**(4): 43-54. https://www.researchgate.net/publication/299559938_Idealised_Bilinear_Moment-Curvature_Curves_of_RC_Sections_for_Pushover_Analysis_of_RC_Frame_Buildings
- 25 Federal Emergency Management Agency (2009). "FEMA P695: Quantification of Building Seismic Performance Factors". Washington, DC, USA. https://nehrpsearch.nist.gov/static/files/FEMA/PB2010101_512.pdf
- 26 Vecchio FJ and Emara MB (1992). "Shear deformations in reinforced concrete frames". *ACI Structural Journal*. **89**(1): 46-56. http://vectoranalysisgroup.com/journal_publications/jp16.pdf
- 27 Applied Technology Council (1996). "ATC-40: Seismic Evaluation and Retrofit of Concrete Buildings". California, USA. <https://www.atccouncil.org/pdfs/atc40toc.pdf>